

ChemComm

Accepted Manuscript



This is an *Accepted Manuscript*, which has been through the Royal Society of Chemistry peer review process and has been accepted for publication.

Accepted Manuscripts are published online shortly after acceptance, before technical editing, formatting and proof reading. Using this free service, authors can make their results available to the community, in citable form, before we publish the edited article. We will replace this *Accepted Manuscript* with the edited and formatted *Advance Article* as soon as it is available.

You can find more information about *Accepted Manuscripts* in the [Information for Authors](#).

Please note that technical editing may introduce minor changes to the text and/or graphics, which may alter content. The journal's standard [Terms & Conditions](#) and the [Ethical guidelines](#) still apply. In no event shall the Royal Society of Chemistry be held responsible for any errors or omissions in this *Accepted Manuscript* or any consequences arising from the use of any information it contains.



ChemComm

COMMUNICATION

A simple and controllable graphene-templated approach to synthesise 2D silica-based nanomaterials using water-in-oil microemulsions

Received 00th January 20xx,
Accepted 00th January 20xx

DOI: 10.1039/x0xx00000x

www.rsc.org/

Yang Xue^a, Yun Sheng Ye^{a*}, Fang Yan Chen^a, Hao Wang^a, Chao Chen^a, Zhi Gang Xue^a, Xing Ping Zhou^a, Xiao Lin Xie^{a*}, Yiu-Wing Mai^b

Using the versatility of silica chemistry, we describe herein a simple and controllable approach to synthesise two-dimensional (2D) silica-based nanomaterials: the diversity and utility of the resulting structures offer excellent platforms for many potential applications.

Nanomaterials are being developed for current and potential applications in many fields, which include energy, medical and biotechnology, owing to their unique optical, electronic and/or mechanical properties. Two-dimensional (2D) nanostructures, owing to their quantum band structures and oriented surface exposure, have properties that are not found in their zero- or one-dimensional counterparts.¹ Interest in 2D nanomaterials received a major boost with the discovery of graphene sheets by Novoselov, Geim and co-workers in 2004.² Since then, other 2D nanomaterials, including various metal chalcogenides (MoS₂, MoO₃, TiSe₂, Bi₂Te₃)³⁻⁶, and insulating hexagonal boron nitride⁷ have become the focus of intensive research, because of their structural similarities to graphene. Silica has generated significant interest as a potentially useful material as a result of its unique properties that include: the ability to form materials with a great variety of structures, precise control of hydrolysis-condensation reactions, and superior thermal stability of silica amorphous networks. Silica nanostructures, especially silica nanoparticles and nanotubes, are of special interest due to their hydrophilicity, simple colloidal suspension formation, easy chemical functionalizability and good compatibility with biomolecules or polymer chains.⁸⁻¹⁰ However, advances in 2D silica nanomaterial applications have been limited caused by the difficulties in synthesis and fabrication of nanostructures with well-controlled dimensions, morphologies, phase purities

and chemical compositions.

A perfect 2D graphene sheet can be used as a template for the assembly or coating of nanoparticles or other 2D silica-based nanomaterials.¹¹ A number of methods have been tried to coat silica nanoparticles on graphene oxide (GO), which include the “loading to”^{12, 13} and “loading from”¹⁴⁻¹⁹ strategies. The “loading to” approach, which involves the preparation of silica nanomaterials prior to coupling, allows full structural and size control, but generally results in a low coupling density with a non-uniform distribution due to the steric hindrance from the attached silica particles and the relatively low reactivity of the functional groups on the surfaces of GO. Conversely, the “loading from” approach promises a relatively high coupling density; however, the formation of silica particles, both free and attached to GO, during coupling reaction is unavoidable, which makes it more difficult to control particle distribution on templated graphene. An insufficient coverage can originate from a lack of chemical affinity between the surface of GO and silica. To address this problem, GO has been functionalized with silicon-ethoxide groups to promote condensation with a silica precursor.¹⁹ A similar strategy was adopted for building homogeneous multi-walled CNT silica nanoparticle composite materials.²⁰⁻²² However, the formation of free silica particles and their condensation with silica particles adhering to the GO surface is still unavoidable. An additional constraint is the fact that at least two processing steps are required using the conventional technologies, which makes the overall procedure complex and inefficient.

GO consists of two types of randomly distributed regions: aliphatic six-member regions, and aromatic regions with non-oxidised benzene rings.²³ In recent studies,²⁴⁻²⁹ it has been shown that GO sheets can act as surfactants or dispersants because of their amphiphilic characteristics and the formation of Langmuir-Blodgett films on water surfaces in the absence of other amphiphilic molecules. All of these studies suggest that the use of GO sheets can stabilize emulsions or mini-emulsions of various solvents and monomers without using additional surfactants. These features enable the GO sheets to serve as

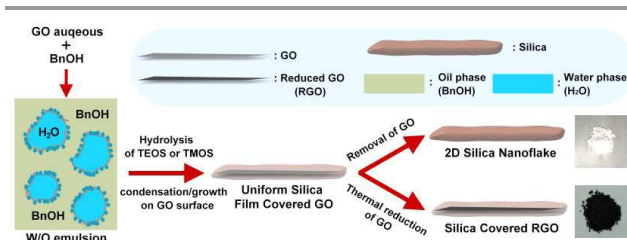
^aKey Laboratory for Large-Format Battery Materials and Systems, Ministry of Education, School of Chemistry and Chemical Engineering, Huazhong University of Science and Technology, Wuhan 430074, China.

^bCentre for Advanced Materials Technology (CAMT), School of Aerospace, Mechanical and Mechatronic Engineering J07, The University of Sydney, Sydney NSW 2006, Australia

† Electronic Supplementary Information (ESI) available: [details of any supplementary information available should be included here]. See DOI: 10.1039/x0xx00000x

surfactants, which can create microemulsions; and be used as templates for preparation of 2D nanomaterials.

Herein, we used GO in a highly controllable, tunable and reproducible synthesis, based on an oil-water biphasic reaction system, to prepare 2D silica-based nanomaterials. Instead of growing the silica nanoparticles on the surface of GO in the EtOH/water co-solvent system, we chose to grow the silica nanoparticles onto the GO surface by reaction with tetraethyl- or tetramethyl- orthosilicate (TEOS or TMOS), using a water-in-oil microemulsion (water/benzyl alcohol; H₂O/BnOH) to control precisely the nanoparticle size and distribution (Scheme 1). Details of the synthesis methodology are provided in the experimental section (ESI[†]). We successfully obtained ultra-thin silica nano-flakes (SiO₂/NF), and thermally reduced GO (TRGO) (uniformly and controllably coated with a silica layer (SiO₂/TRGO)), by heat treatment at 700 °C in air and in a 5 wt.% H₂/Ar atmosphere, respectively. The distinct advantage of this strategy compared to approaches adopted in previous reports is that the absence of free silica particles during sol-gel processing makes it simple and easy to implement.



Scheme 1. A schematic of the process adopted for synthesis of silica nano-flake and silica-covered RGO.

The silica coating mechanism on the GO surface was characterized using SEM, TEM, XRD and TGA. The TEM images shown in Fig. 1(a) reveal that hetero-nucleated silica seeds (<10 nm diameter, shown as dark regions in TEM images and light regions in SEM images) were evenly anchored on the GO surface by condensation of silicic acid with protic functional groups of GO after reaction for 4 h. Subsequently, (after 24 h), more and more parasitic silica particles grew laterally on the surface of the GO, resulting in evenly and densely covered GO sheets. Under higher magnification, the average diameter of the covered silica was ca. 20 nm. The unambiguous shapes and interconnects of the silica particles were clearly visible and found to be much smaller than those of silica particles covered by GO prepared in an EtOH/water system (~50 nm).¹⁴ In addition, as silica growth is effectively localized on the GO surface and the sol-gel reaction only occurs in the surrounding water phase, no free silica particles are generated within the substrate (wafer) (Fig. S1); thus centrifugation to remove silica particles is not required.

XRD and TGA results reflect the degree of silica coverage and amount of silica formed on the surface of GO. As shown in Fig. 1(b), the peak at $2\theta = 9.89^\circ$, corresponding to the X-ray reflection of the (002) planes of GO,³⁰ obviously weakens after 4 h and is almost completely gone at 8 h. This result indicates that the regular stacks of GO were destroyed by silica coverage

on the surfaces of GO sheets. The homogeneous silica growth mechanism allowed regular stacks of GO to be destroyed, even after a short reaction time (stacks of GO were destroyed after 24 h in the EtOH/water system¹⁴). The TGA result [Fig. 1(c)] shows that the normalized residual yield of SiO₂(TEOS)/GO at 800 °C increased with increasing reaction times, indicating that silica particles became increasingly loaded on GO sheets with time. A kinetic study of silica covered GO nanohybrids was carried out by graphically fitting the weight of loaded silica at different reaction states as a linear function, namely ($\ln W = 0.5505 \times \ln T + 0.2843$; where $\ln T$ and $\ln W$ designate the natural logarithms of reaction time and loaded silica weight, respectively).

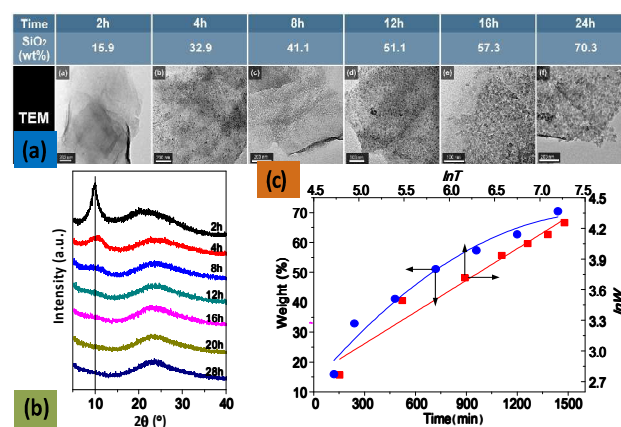


Fig. 1 (a) TEM images and (b) XRD pattern of SiO₂(TEOS)/GO; and (c) normalized residual weight of SiO₂(TEOS)/GO at 800 °C as a function of reaction time (blue line). Corresponding natural logarithm of normalized residual weight ($\ln W$) in TGA measurements as a function of natural logarithm of reaction time ($\ln T$).

The degree of silica coverage and the amount of silica formation on the GO surface were also examined by adjusting the amounts of reagents. Fig. 2 (top row) shows SEM and TEM micrographs of SiO₂(TEOS)/GO where the amount of reactants is varied (molar/weight ratio of TEOS to GO is increased from 10.8 to 53.9). At low TEOS/GO ratios, parts of the GO surface are not sufficiently coated with silica. Above the molar/weight ratio [TEOS]/[GO] = 43.1, GO surfaces are fully covered by uniform silica layers as shown in Figs. 2 top row, (d) and (e). The average diameter of silica particles on SiO₂(TEOS)/GO is summarized in Table 1, which shows the average diameter increases slightly with the concentration of TEOS. It is notable that free silica particles are not produced under the testing conditions used. These results indicate that GO is instantly coated with small silica (SiO₂) particles upon generation owing to the confined surface condensation reaction, as illustrated in Fig. 3 bottom. In contrast to the growth of silica nanoparticles on the surface of GO in the EtOH/water co-solvent system, here the silica layers on GO surface and the free silica particles form simultaneously.³¹ These free silica particles are able to condense with the silica layers of GO, resulting in non-uniform SiO₂ particles covering the GO surface, as illustrated in Fig. 3 top.

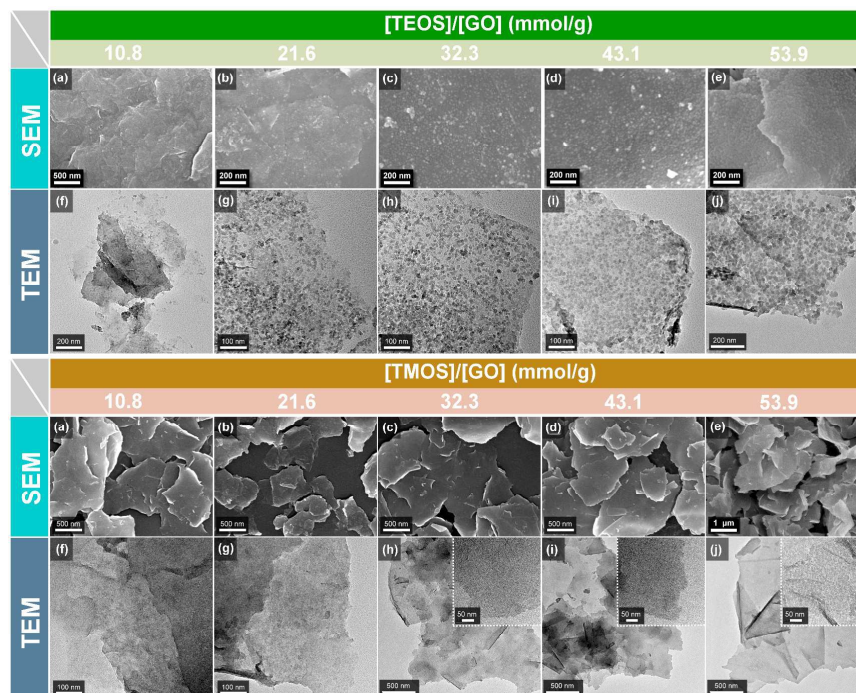


Fig. 2 SEM and TEM images of $\text{SiO}_2(\text{TEOS})/\text{GO}$ and $\text{SiO}_2(\text{TMOS})/\text{GO}$ synthesized at different molar/weight ratios of $[\text{TEOS}]/[\text{GO}]$.

Table 1. Variation of SiO_2/GO average diameter prepared with an increasing amount of TEOS with a fixed weight of ($\text{NH}_4\text{OH} = 1.96 \text{ g}$).

Samples	GO (g)	TEOS (mmol)	$[\text{TEOS}]/[\text{GO}]$ (mmol/g)	Average diameter (nm) ^a
A	0.30	3.23	10.8	7.7
B	0.30	6.46	21.6	9.9
C	0.30	9.69	32.3	12.0
D	0.30	12.92	43.1	15.3
E	0.30	16.15	53.9	19.1

^a Calculated from TEM (100 particles were randomly selected as calculating).

We also studied the effect of the hydrolysis/condensation rate of the silane precursor on the morphology of organosilicas by replacing TEOS with TMOS. SEM and TEM micrographs of $\text{SiO}_2(\text{TMOS})/\text{GO}$ (Fig. 2 bottom) show that the morphology of SiO_2/GO prepared by TMOS is different from $\text{SiO}_2(\text{TEOS})/\text{GO}$, which has a non-spherical morphology upon covering the GO surface. The $\text{SiO}_2(\text{TMOS})/\text{GO}$ samples are mainly composed of homogeneous silica layers on the surface of GO under any of the testing conditions explored, even at low concentrations of TMOS ($[\text{TMOS}]/[\text{GO}] = 10.8 \text{ mmol/g}$). We speculated that this silane precursor has a fast hydrolysis rate and can thus rapidly generate more hydrolyzed silica species to condense with GO-supported hetero-nucleated silica, thereby leading to the formation of highly interconnected silica of a larger uniformity covering the GO surface, as compared to material made using the silane precursor of TEOS (Fig. S2).

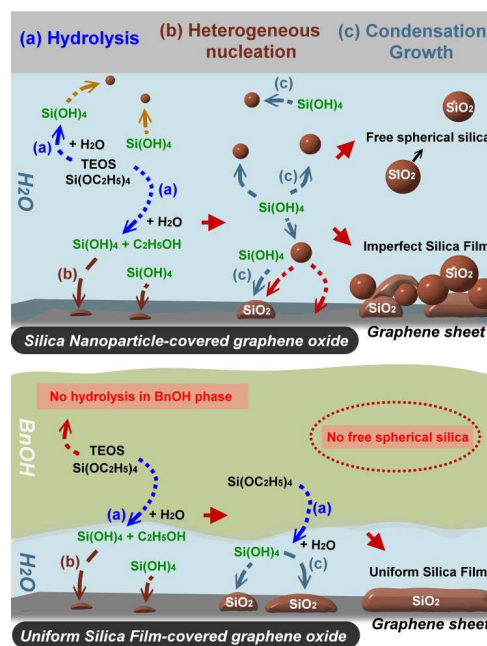


Fig. 3 Sequence of growing silica film on GO surface in EtOH/water co-solvent and water/BnOH biphasic systems. Details of the mechanism are described in the ESI†.

SiO_2/TRGO and SiO_2/NF were prepared by thermal reduction and calcination at 700°C under a 5 wt.% H_2/Ar atmosphere and in air, respectively. After removal of the GO templates, SiO_2/NF were self-supporting with the average size of $1\sim 4 \mu\text{m}$ (Fig. S3). The TGA result (Fig. S4) shows that a coating of silica on the surface of TRGO caused a dramatic

increase in the onset of weight loss relative to the thermal oxidative decomposition of carbon, indicating that the homogeneous and condensed silica layer acts as a protective barrier preventing oxidative degradation. The SiO₂/NF had a high thermal stability, with almost no obvious mass loss up to 800 °C. The variations in surface composition for GO, SiO₂/GO and SiO₂/TRGO were investigated by XPS, Fig. S5. The peaks at approximately 533.4, 532.6 and 103.6 eV in the curve fitting of the O1s and Si2p indicate the formation of a silica network, while the peaks at 531.7 and 103.0 eV provide evidence of covalent bonding between GO and silica. This result is in good agreement with the FTIR data (Fig. S6). After the thermal reduction process, the intensities of C-O and C=O peaks in the C1s spectra decrease dramatically due to the elimination of significant amounts of oxygen-containing functional groups from GO during thermal treatment, which turns the inner GO of the SiO₂/GO into TRGO. Raman spectra (Fig. S7) of GO, SiO₂/GO and SiO₂/TRGO show a D-band at ~1349 cm⁻¹ and a G-band at ~1593 cm⁻¹, corresponding to the stretching modes of sp² and sp³ hybridized carbon, respectively. There is no obvious change in the intensity ratio (*I_D/I_G*) for silica-covered TRGO, which is consistent with most thermal reduction results at the same temperature.^{32, 33} For SiO₂/NF, the absence of apparent peaks indicates that the inner GO of SiO₂/GO is successfully removed and transformed to silica nanoflakes during pyrolysis in an air atmosphere.

In conclusion, we employed a highly controllable, tunable and reproducible synthesis using a water-in-oil micro-emulsion approach to prepare 2D silica-based nanomaterials. The most valuable feature of this work is that the architecture of the obtained nanomaterials can be precisely controlled without creating any free silica particles during the sol-gel process. Versatile chemical properties can be introduced into the silica-based nanomaterials surface by doping with drugs, biocides, metal or metal nitride, nanomaterials with a wide range of functionalities suitable for different applications.³⁴ Moreover, the versatility of this approach can be extended to other oxides and thus may be used to build other 2D-functional nanocomposites. Overall, the synthetic strategy proposed in this study is simple, easy and controllable, and opens a new avenue for the synthesis of 2D silica-based nanomaterials in an effective and facile manner.

The authors acknowledge the financial support of this work by the National Natural Science Foundation of China (51210004 and 51503071), and the analytical and testing assistance from the Analysis and Testing Center of HUST.

Notes and references

1. E. L. Tae, K. E. Lee, J. S. Jeong and K. B. Yoon, *J. Am. Chem. Soc.*, 2008, **130**, 6534-6543.
2. K. S. Novoselov, A. K. Geim, S. V. Morozov, D. Jiang, Y. Zhang, S. V. Dubonos, I. V. Grigorieva and A. A. Firsov, *Science*, 2004, **306**, 666-669.
3. N. Liu, P. Kim, J. H. Kim, J. H. Ye, S. Kim and C. J. Lee, *ACS Nano*, 2014, **8**, 6902-6910.
4. D. Hanlon, C. Backes, T. M. Higgins, M. Hughes, A. O'Neill, P. King,

- N. McEvoy, G. S. Duesberg, B. Mendoza Sanchez, H. Pettersson, V. Nicolosi and J. N. Coleman, *Chem. Mater.*, 2014, **26**, 1751-1763.
5. L. Ren, X. Qi, Y. Liu, G. Hao, Z. Huang, X. Zou, L. Yang, J. Li and J. Zhong, *J. Mater. Chem.*, 2012, **22**, 4921-4926.
6. K. J. Koski and Y. Cui, *ACS Nano*, 2013, **7**, 3739-3743.
7. Y. Lin and J. W. Connell, *Nanoscale*, 2012, **4**, 6908-6939.
8. X. Yang, H. Tang, K. Cao, H. Song, W. Sheng and Q. Wu, *J. Mater. Chem.*, 2011, **21**, 6122-6135.
9. T. Yu, A. Malugin and H. Ghandehari, *ACS Nano*, 2011, **5**, 5717-5728.
10. I. A. Rahman and V. Padavettan, *J. Nanomater.*, 2012, **2012**, 2817-2827.
11. Y.-F. Lee, K.-H. Chang and C.-C. Hu, *Chem. Commun.*, 2011, **47**, 2297-2299.
12. K. Feng, B. Tang and P. Wu, *J. Mater. Chem. A*, 2014, **2**, 16083-16092.
13. T. Jiang, T. Kuila, N. H. Kim and J. H. Lee, *J. Mater. Chem. A*, 2014, **2**, 10557-10567.
14. L. Kou and C. Gao, *Nanoscale*, 2011, **3**, 519-528.
15. S. Choi, K. Kim, J. Nam and S. E. Shim, *Carbon*, 2013, **60**, 254-265.
16. Z. Lu, J. Zhu, D. Sim, W. Zhou, W. Shi, H. Hng and Q. Yan, *Chem. Mater.*, 2011, **23**, 5293-5295.
17. M. C. Hsiao, C. C. M. Ma, J. C. Chiang, K. K. Ho, T. Y. Chou, X. Xie, C. H. Tsai, L. H. Chang and C. K. Hsieh, *Nanoscale*, 2013, **5**, 5863-5871.
18. L. Kan, B. Zheng and C. Gao, *Chin. Sci. Bull.*, 2012, **57**, 3026-3029.
19. X. Pu, H. B. Zhang, X. Li, C. Gui and Z. Z. Yu, *RSC Adv.*, 2014, **4**, 15297-15303.
20. K. Babooram and R. Narain, *ACS Appl. Mater. Interfaces*, 2009, **1**, 181-186.
21. M. Bottini, L. Tautz, H. Huynh, E. Monosov, N. Bottini, M. I. Dawson, S. Bellucci and T. Mustelin, *Chem. Commun.*, 2005, **6**, 758-760.
22. Y. Liu, C. Zhang, Z. Du, C. Li, Y. Li, H. Li and X. Yang, *Carbon*, 2008, **46**, 1670-1677.
23. D. R. Dreyer, S. Park, C. W. Bielawski and R. S. Ruoff, *Chem. Soc. Rev.*, 2010, **39**, 228-240.
24. Y. Cao, J. Zhang, J. Feng and P. Wu, *ACS Nano*, 2011, **5**, 5920-5927.
25. J. M. Thomassin, M. Trifkovic, W. Alkarmo, C. Detrembleur, C. Jérôme and C. Macosko, *Macromolecules*, 2014, **47**, 2149-2155.
26. L. J. Cote, F. Kim and J. Huang, *J. Am. Chem. Soc.*, 2009, **131**, 1043-1049.
27. C. Zhang, L. Ren, X. Wang and T. Liu, *J. Phys. Chem. C.*, 2010, **114**, 11435-11440.
28. L. Tian, M. J. Meziani, F. Lu, C. Y. Kong, L. Cao, T. J. Thorne and Y. P. Sun, *ACS Appl. Mater. Interfaces*, 2010, **2**, 3217-3222.
29. L. Qiu, X. Yang, X. Gou, W. Yang, Z.-F. Ma, G. G. Wallace and D. Li, *Chem. Euro. J.*, 2010, **16**, 10653-10658.
30. Y. S. Ye, Y. N. Chen, J. S. Wang, J. Rick, Y. J. Huang, F. C. Chang and B. J. Hwang, *Chem. Mater.*, 2012, **24**, 2987-2997.
31. W. L. Zhang and H. J. Choi, *Langmuir*, 2012, **28**, 7055-7062.
32. C. Botas, P. Álvarez, C. Blanco, R. Santamaría, M. Granda, M. D. Gutiérrez, F. Rodríguez-Reinoso and R. Menéndez, *Carbon*, 2013, **52**, 476-485.
33. N. J. Song, C. M. Chen, C. Lu, Z. Liu, Q. Q. Kong and R. Cai, *J. Mater. Chem. A*, 2014, **2**, 16563-16568.
34. R. Ciriminna, A. Fidalgo, V. Pandarus, F. Béland, L. M. Ilharco and M. Pagliaro, *Chem. Rev.*, 2013, **113**, 6592-6620.